Absorbance Detected Magnetic Resonance Spectra of the FMO Complex of *Prosthecochloris aestuarii* Reconsidered: Exciton Simulations

Gabrielle M. Owen and Arnold J. Hoff*

Department of Biophysics, Huygens Laboratory, Leiden University, P.O. Box 9504, 2300 RA Leiden, The Netherlands

Received: August 30, 2000; In Final Form: December 7, 2000

The isotropic and linear dichroic triplet−singlet difference spectra of the Fenna−Matthews−Olson (FMO) complex of the green sulfur bacterium *Prosthecochloris aestuarii* measured with absorbance detected magnetic resonance (ADMR) are presented. The absorption, linear dichroic (LD), circular dichroic (CD), triplet-minus-singlet (T−S), and LD(T−S) spectra are simultaneously analyzed by means of an exciton model. In this analysis the dependence of the T−S(α) spectrum on the angle α between the optical and microwave transition moments was taken into account. The present simulation procedure yields fits of the absorption and LD spectra of FMO that are about equally good as those in the literature, while the fits of the CD, T−S, and LD(T−S) spectra show significant improvements. We find that the interaction energies are roughly 25% higher than in previous analyses. The simultaneous fit of all available optical (difference) spectra with correct procedures offers a precise and detailed description of pigment−pigment interactions in the FMO complex.

Introduction

With the advent of the crystal structures of a number of photosynthetic reaction center and light-harvesting pigment−protein complexes, there is a strong interest in the interpretation and simulation of their optical spectra by exciton theory, combined or not with various quantum-chemical calculations. A particularly interesting case is the Fenna−Matthews−Olson (FMO) water-soluble BChl *a* complex of the green sulfur bacterium *Prosthecochloris* (*P.*) *aestuarii*, whose crystal structure is known to 1.9 Å resolution.[1] The complex consists of three identical subunits arranged in C_3 symmetry. Each subunit contains seven BChl *a* molecules. For some time, its various optical spectra, such as absorbance and linear and circular dichroic (LD, CD) spectra, resisted consistent interpretation.[2−4] Optically detected magnetic resonance (ODMR) was recently used to further investigate the FMO complex.[5] ODMR is a technique used to measure the change in an optical property due to microwave-induced transitions between magnetic sublevels of the lowest triplet state. The three branches of ODMR are named after the commonly monitored optical properties: absorbance (ADMR), fluorescence (FDMR), and phosphorescence (PDMR). Various types of triplet-minus-singlet (T−S) spectra can be measured with ODMR. The different T−S spectra show the subtle differences of the optical properties of the system in the singlet and triplet states, from which intermolecular distances, relative orientations, and couplings can be determined.

The T−S spectrum is the difference of the absorbance with and without the presence of a triplet, and likewise, the double difference linear dichroic T−S (LD(T−S)) spectra are the difference of the LD with and without the presence of a triplet. Thus, the singlet part of the T−S spectra at a fixed microwave frequency is a selected subset of the singlet absorbance measured with conventional absorption spectroscopy. Note that the angle between the optical and microwave transition moments is derived from the ratio of the LD(T−S) signal to the T−S signal at low microwave powers, whereas the angle between the optical transition moment and the membrane normal or symmetry axis of the sample is derived from the ratio of the LD to the absorbance signal. Both of these angles can be used to help derive the structure of the examined molecule and to definitely assign bands in the T−S spectra.

It was shown that by taking into consideration T−S and linear dichroic T−S (LD(T−S)) absorbance difference spectra recorded with ADMR, simultaneous simulation of all optical spectra of the FMO complex narrowed the parameter space considerably and yielded acceptable fits of all spectra.[5] However, the T−S spectrum presented in ref 5 is the sum of the change in absorbance of light polarized parallel and perpendicular to the polarization of the microwave field employed in ADMR. This T−S spectrum, which we denote as T−S(α), is dependent on the angle α between the optical and microwave transition moments, but was simulated as an α-independent T−S spectrum.[6] These observations have prompted us to reinvestigate the optical spectra of the FMO complex.

We make use of the T−S(α) and LD(T−S) spectra and their ratio on an isolated band from ref 7 to derive the isotropic T−S spectrum, defined as the change in absorbance of light polarized parallel plus twice the change in absorbance perpendicular to the polarization of the microwave field. The optical spectra are simulated similarly as in ref 5, giving the energies, effective dipole strengths, and wave functions of the FMO complex of *P. aestuarii*. For a fixed exciton bandwidth of 80 cm^{-1} as in ref 5, we find significantly better spectral fits than those of ref 5. We conclude that simultaneous fitting of all available optical (difference) spectra with correct procedures offers a precise, detailed description of pigment−pigment interactions in a pigment−protein complex.

Materials and Methods

2.1 Experimental Spectra. The experimental LD and CD spectra of the FMO complex of *P. aestuarii* are taken from refs

* Corresponding author. Telephone: +31 71 5275955. Fax: +31 71 5275819. e-mail: hoff@biophys.leidenuniv.nl

10.1021/jp0031247 CCC: $20.00
Published on Web 01/26/2001

8 and 9, respectively. The absorption, and ADMR-detected T−S(α) and LD(T−S) spectra are from ref 7.

As explained in ref 6, the ADMR-detected T−S(α) spectra of ref 7, which were measured under nonsaturating conditions, are dependent on the angle α between the electric transition dipole moment of the optical transition and the microwave transition moment of a zero-field transition of the triplet. Isotropic, α-independent ADMR-detected T−S spectra are equal to $\Delta A_V(\lambda)$ plus *twice* $\Delta A_H(\lambda)$, where $\Delta A_V(\lambda)$ and $\Delta A_H(\lambda)$ are the changes in absorption of light polarized parallel and perpendicular to the polarization of the applied magnetic field.[6] T−S(α) spectra are the sum of $\Delta A_V(\lambda)$ and $\Delta A_H(\lambda)$. The T−S spectra are derived from the T−S(α) and LD(T−S) spectra of ref 7 by first scaling the spectra with the measured R-ratio at 827 nm[7] and then using the formula[6]

$$\Delta A_{\mathrm{T-S}}(\lambda) = \frac{3}{2}\Delta A_{\mathrm{T-S(\alpha)}}(\lambda) - \frac{1}{2}\Delta A_{\mathrm{LD(T-S)}}(\lambda) \tag{1}$$

The R-ratio for an isolated band is defined as

$$R = \frac{\mathrm{LD(T-S)}}{\mathrm{(T-S)(\alpha)}} = \frac{\Delta A_V - \Delta A_H}{\Delta A_V + \Delta A_H} = \frac{3\cos^2\alpha - 1}{3 + \cos^2\alpha} \tag{2}$$

The integrated area of the long-wavelength band at 827 nm in the T−S spectrum was set equal to the integrated area of the band at 825 nm in the absorption spectrum, because both bands most probably stem from the triplet-carrying BChl. The LD-(T−S) spectrum of each zero-field transition is scaled to the absorption spectrum on the 827 nm band by the factor 2R/(R−3). The scales for the LD and CD spectra are left arbitrary. The experimental T−S and LD(T−S) spectra were translated 2 nm to the blue to correspond with the absorption spectrum. It has been shown that the position of the bands in the T−S spectra can change a few nm according to the applied microwave frequency.[10] This effect is caused by inhomogeneous broadening of the absorption bands and selective excitation of the microwave transition.[11]

2.2 Simulation Procedure. We analyze the experimental data with an excitonic model, which has been described previously.[12,13] In the Hamiltonian H, used in the exciton model, each pigment is specified by an index n, a diagonal energy E_n, and an interaction matrix element V_{mn}:

$$H = \sum_{n=1}^{N} |n\rangle\, E_n\, \langle n| + \sum_{n\neq m}^{N} |m\rangle\, V_{mn}\, \langle n| \tag{3}$$

The interaction matrix element V_{mn}, also known as the dipolar coupling term, is for point dipoles:

$$V_{mn} = V_{nm} = \frac{5.04\kappa_{mn}|\mu_m||\mu_n|}{\eta^2 R_{mn}^3} \tag{4}$$

where the magnitudes of the transition dipole vectors $|\mu_m|$, $|\mu_n|$ are given in Debye, the distance R_{mn} between the two dipoles is given in nm, V_{mn} is given in cm^{-1}, and η is the ratio of the permittivity to that in free space.[14,15] The point-dipole approximation is valid because of the large average distances between the pigments (ranging between 11.3 and 14.4 Å). The orientation factor κ_{mn} for the dipole−dipole interaction is:

$$\kappa_{mn} = (\hat{\mu}_m\hat{\mu}_n) - 3(\hat{\mu}\hat{r}_{mn})(\hat{\mu}_n\hat{r}_{mn}) \tag{5}$$

where (ˆ) denotes a unit vector. We diagonalize H to find the eigenvectors and eigenvalues. The procedure is performed for the Hamiltonians that describe the interactions with and without a triplet present. The eigenvalues are the energies $\hbar\omega^{(k)}$ ($k = 1,...,N$), and the eigenvectors are denoted as $e^{(k)} = (e_1^{(k)} ..., e_N^{(k)})$. The corresponding transition moments $\nu^{(k)}$ are linear combinations of the transition dipole moment vectors $\mu^{(n)}$ of the isolated pigments weighted by the eigenvector components $e_n^{(k)}$ as follows:

$$\nu^{(k)} = \sum_{n=1}^{N} e_n^{(k)}\mu^{(n)} \tag{6}$$

The resulting eigenvectors show that the states of the coupled system are delocalized over the individual pigments.

The absorbance, linear dichroic, and the circular dichroic spectra are calculated according to respectively. In these

$$A = c\sum_{k=1}^{N} A_k = \sum_{k=1}^{N} (\nu^{(k)})^2 \rho_k(\omega_\lambda) \tag{7}$$

$$\Delta A_{\mathrm{LD}} = A_{\parallel} - A_{\perp} = \frac{3}{2}\sum_{k=1}^{N} A_k(1 - 3\cos^2\phi_k) \tag{8}$$

$$\Delta A_{\mathrm{CD}} = 1.7 \times 10^{-5}\sum_{k=1}^{N} \hbar\omega^{(k)}\rho_k(\omega_\lambda)\sum_{i,j=1}^{N} \vec{\mu}^{(i)}\vec{R}_{ij} \times \vec{\mu}^{(j)} e_i^{(k)} e_j^{(k)} \tag{9}$$

equations, c is a constant, ϕ is the angle between the optical dipole moment and the C_3 axis of the trimer, $\rho_k(\omega_\lambda)$ is a line-shape factor, and ω_λ is the frequency of the light.

The T−S spectrum is simulated with:

$$\Delta A_{\mathrm{T-S}}(\lambda) = \Delta A_V(\lambda) + 2\Delta A_{\mathrm{H}}(\lambda) \tag{10}$$

$$= \sum_{k=1}^{N} [|{}^T\nu_{Sk}|^2 \rho_k(\omega_\lambda) + |\nu_{Tk}|^2 \rho_k(\omega_\lambda) - |\nu_{Sk}|^2 \rho_k(\omega_\lambda)] \tag{11}$$

where $|{}^T\nu_{Sk}|$ and $|\nu_{Sk}|$ are the magnitudes of the dipole moments of the $S_1 \leftarrow S_0$ transition with and without a pigment in the triplet state, respectively, and $|\nu_{Tk}|$ is the magnitude of the dipole moment of the $T_1 \leftarrow T_0$ absorption. The LD(T−S) spectrum is simulated according to ref 6:

$$\Delta A_{\mathrm{LD(T-S)}}(\lambda) = \Delta A_V(\lambda) - \Delta A_H(\lambda) \tag{12}$$

$$= 1/5\sum_{k=1}^{N} [|{}^T\nu_{Sk}|^2 \rho_k(\omega_\lambda)(3\cos^2({}^T\alpha_{Sk}) - 1) + |\nu_{Sk}|^2 \rho_k(\omega_\lambda)(3\cos^2\alpha_{Tk} - 1) - |\nu_{Tk}|^2 \rho_k(\omega_\lambda)(3\cos^2\alpha_{Sk} - 1)] \tag{13}$$

where ${}^T\alpha_{Sk}$, α_{Sk}, α_{Tk} are the angles between the optical and microwave transition moments for ${}^T\vec{\nu}_{Sk}$, $\vec{\nu}_{Sk}$, $\vec{\nu}_{Tk}$, respectively.

2.3 Parameter Choice. The calculation of the transition dipole moments $\nu_S^{(k)}$ and energies $\hbar\omega_S^{(k)}$ for the singlet state of the coupled system is straightforward. The directions of the transition dipole moments $\mu^{(n)}$ are chosen to be along the line connecting the nitrogen atoms of the pyrrole rings I and III (II and IV) for the Q_y (Q_x) bands of the BChl molecules.[16] A dipole strength of 68.9 D^2 is used for the BChls.[17,18] The coupling constants V_{nm} are calculated with eq 4, using the distances and orientations of the pigments from the crystal structure[1] (Brookhaven National Databank, filename 4bchl.pdb). The site

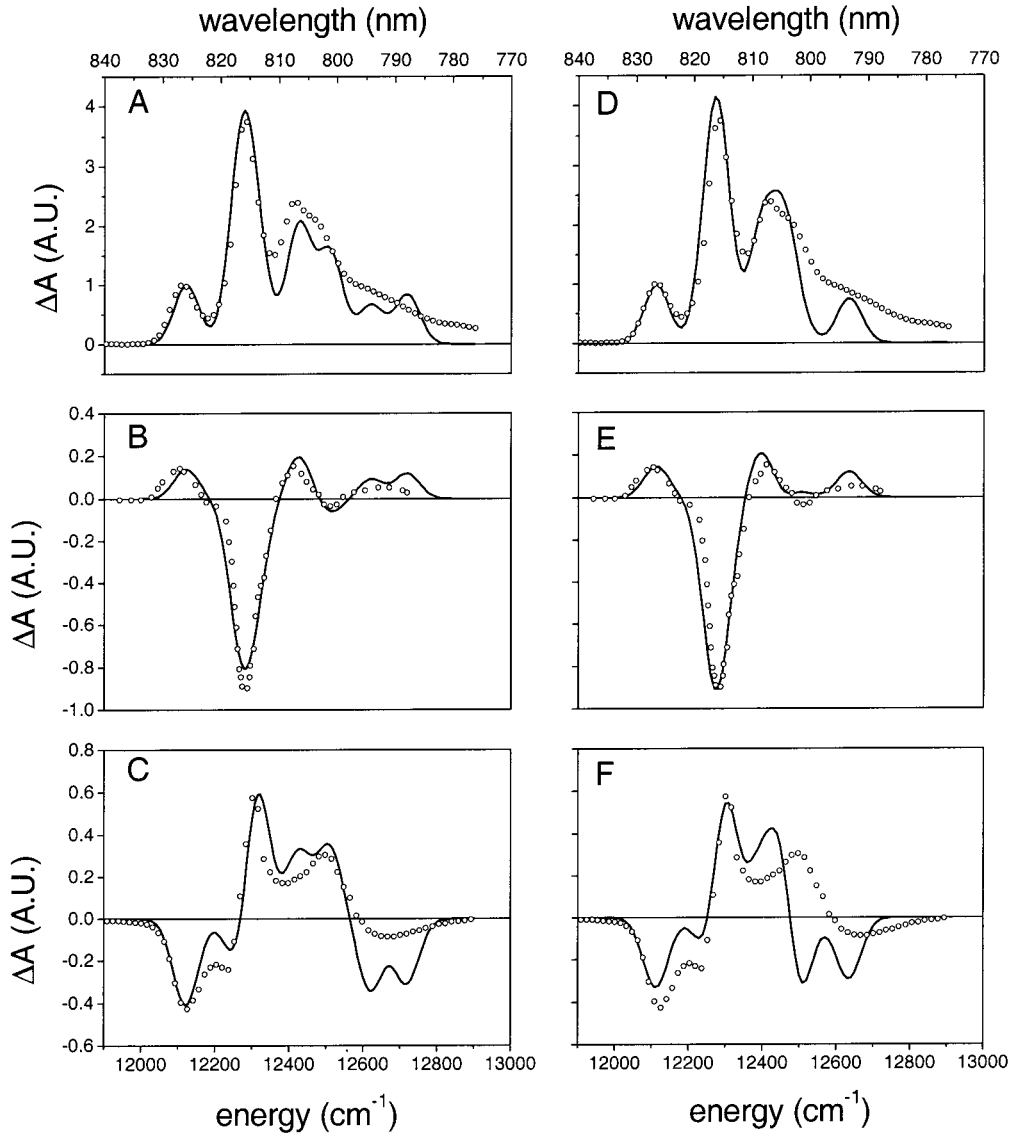

Figure 1. Experimental optical spectra (circles) of the FMO complex of *P. aestuarii* and simulated spectra (solid lines) using the parameter set of Tables 3 and 4 (Figures 1A − 1C) and that of ref 5 (Figures 1D−F). In (A and D) the absorption spectrum (data from ref 7) is shown. In (B and E) the LD spectrum (data from ref 8) is shown. In (C and F) the CD spectrum (data from ref 9) is presented.

energies and the parameter η are left as free parameters. We consider only a single subunit of the FMO complex because the intersubunit interactions are of minor importance.[5] The stick spectra are dressed Gaussian line profiles with line widths equal to 80 cm^{-1}.[19]

When calculating the Hamiltonian that describes the interactions with a triplet present, we assume that the triplet excitation is confined to BChl 3.[7] We assume that there is no interaction between BChl 3 in the triplet state and the other pigments. The directions of the triplet *x* and *y* axes are chosen in the plane of the BChl molecule.

Results

The simulated and experimental absorption, LD, and CD spectra are shown in Figure 1 (left side) together with the corresponding spectra of ref 5 (right side). Similarly, on the left side of Figure 2 the simulated and experimental T−S and LD(T−S) spectra for the $|D| - |E|$ and $|D| + |E|$ transitions are shown, and on the right side, the previously published simulated and experimental T−S(α) and LD(T−S) spectra.

The sum of the squares of the deviations between the experimental and simulated spectra in Figure 1A−F and Figure 2A−F, normalized by the number of points, is given in Tables 1 and 2, respectively. For the LD(T−S) spectra, we additionally correct for the difference in scaling between the left and the right sides of Figure 2, to allow for a fair comparison of the

TABLE 1: Sum of Squares of Deviations between Experimental Data and Fit, normalized by the Number of Points

figure	value	figure	value
1A	0.1037	1D	0.2075
1B	0.0060	1E	0.0138
1C	0.0143	1F	0.0327

TABLE 2: Sum of Squares of Deviations between Experimental Data and Fit, Normalized by the Number of Points[a]

figure	value	figure	value
2A	0.0100	2D	0.0328
2B	0.0015	2E	0.0075
2C	0.0016	2F	0.0044

[a] Because the data in Figure 2B and C are scaled differently than in Figure 2E and F, the values for Figure 2B and C are additionally normalized by the square of the scaling factor.

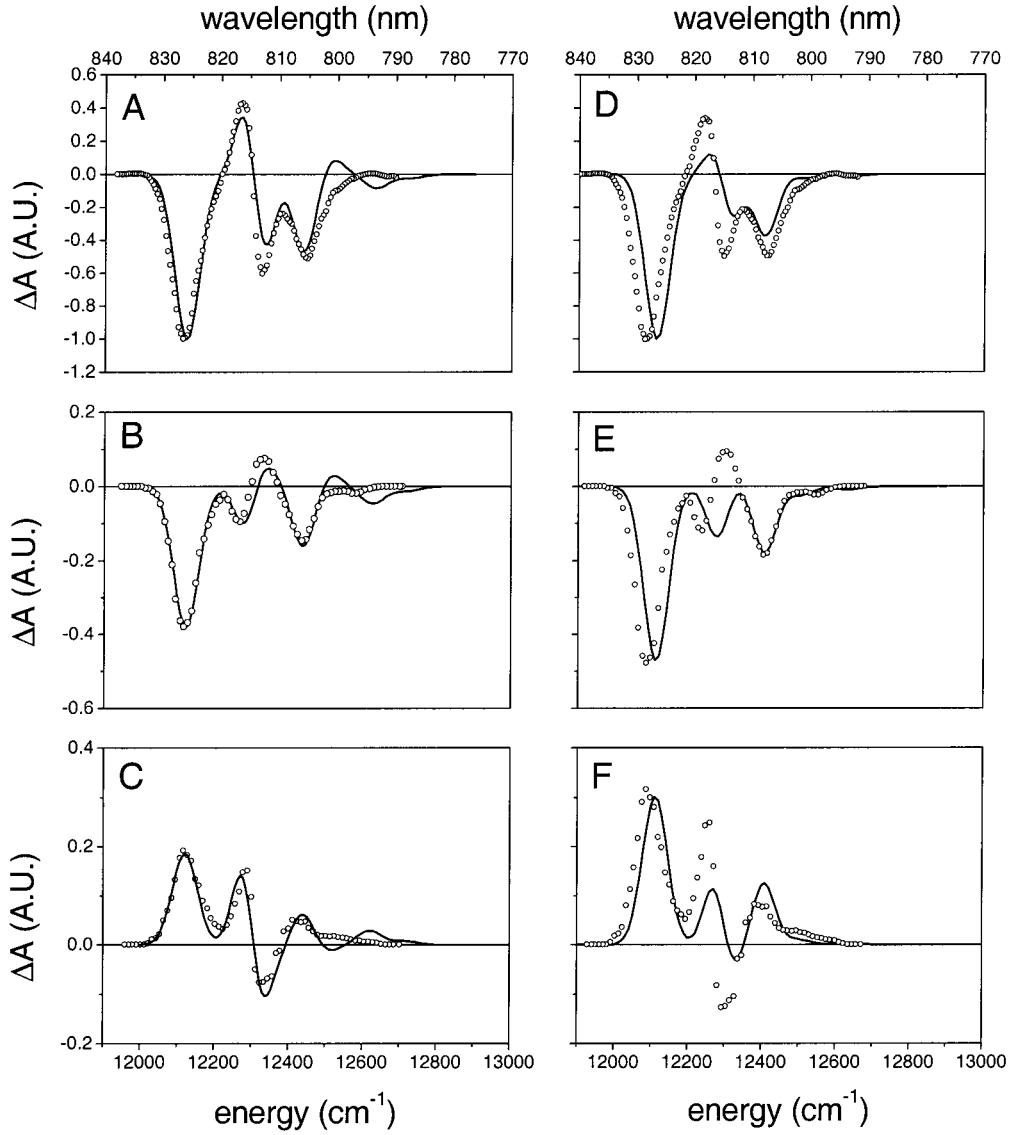

Figure 2. Experimental optical spectra (circles) of the FMO complex of *P. aestuarii* (data from ref 7 or derived from ref 7) and the simulated spectra (solid lines) using the parameter set of Tables 3 and 4 (Figures 2A−C) and that of ref 5 (Figures 2D−F). In (A) the T−S spectrum (experimental points calculated with data from ref 5) is shown. In (B and E) the LD(T−S) spectrum for the $|D| - |E|$ transition is shown. In (C and F) the LD(T−S) spectrum for the $|D| + |E|$ transition is presented. In (D) the T−S(α) spectrum is shown. The lowest energy bands in the experimental LD(T−S) spectra in B and C are scaled to the corresponding bands in the T−S spectrum by the factor $2R/(R - 3)$, those of the experimental LD(T−S) spectra in E and F to the corresponding bands in the T−S(α) spectrum by the factor R.

statistics. Tables 1 and 2 show the improvements of the fits in Figure 1A−C and Figure 2B−C over those in Figure 1D−F and Figure 2E−F, respectively. Note that the data is different in Figures 2A and 2D, so the statistics for these fits are not compared. The absorption spectrum in Figure 1A is well fit in the red part, but the quality of the fit is lower in the blue part. The discrepancies are probably due to the choice of a line width of 80 cm^{-1} and exclusion of vibrational bands (vibronic coupling). A line width of 110 cm^{-1} was found for the 790 nm band,[20] but we fixed the line width to the former value to keep the number of parameters to a minimum, thus facilitating comparison with the treatment of ref 5.

The LD spectrum in Figure 1B is well fit throughout the presented spectral region. Although the major peaks of the CD spectrum in Figure 1C appear in the correct positions, the area of the 12 332 cm^{-1} peak in the fit is less intense than that of the experiment, whereas the band at 12 425 cm^{-1} in the fit is somewhat more intense in the experimental data. Apart from that, the fit is very accurate in the red part, but in the blue part, the fit of the two bands at highest energy is more intense than

TABLE 3: Site Energies and Interaction Energies in cm^{-1} for BChl 1−7

BChl	site energy (cm^{-1})	interaction energy (cm^{-1})						
		1	2	3	4	5	6	7
1	12322		−120	7	−7	9	−18	−16
2	12564	−120		37	10	2	16	10
3	12150	7	37		−65	−2	−12	3
4	12337	−7	10	−65		−81	−22	−70
5	12644	9	2	−2	−81		105	−5
6	12481	−18	16	−12	−22	105		43
7	12477	−16	10	3	−70	−5	43	

the bands in the experimental spectrum. This difference may be due to their low intensity and poor resolution or to the use of a fixed line width. The fit of the T−S spectrum in Figure 2A is less intense than the bands at 12 270 cm^{-1} and 12 322 cm^{-1} in the experimental spectrum. Also here, minor differences exist in the long-wavelength region. In the LD(T−S) spectrum for the $|D| - |E|$ transition (Figure 2B) the fit is very good except for the band at 12 330 cm^{-1}. In the LD(T−S) spectrum

TABLE 4: Excited State Energies E_k, Dipole Strengths (μ^2), and Eigenvectors with and without a Triplet on BChl 3

Without Triplet on BChl 3

		contribution of BChl no.						
E_k cm^{-1} (nm)	μ^2 (D^2)	1	2	3	4	5	6	7
12121 (825.0)	45.9	−0.080	−0.110	**0.932**	0.325	0.051	0.029	−0.054
12270 (815.0)	147.4	**0.895**	0.349	0.023	0.242	0.021	0.039	−0.128
12310 (812.3)	58.0	−0.218	−0.089	−0.329	**0.773**	0.255	−0.188	−0.372
12425 (804.8)	92.1	−0.043	−0.101	−0.131	0.340	−0.284	**0.844**	0.250
12509 (799.4)	70.5	−0.010	0.174	−0.030	0.259	0.312	−0.240	**0.864**
12620 (792.4)	30.2	−0.379	**0.901**	0.062	0.029	−0.137	0.077	−0.122
12718 (786.3)	38.1	−0.024	0.072	0.019	−0.232	**0.858**	0.432	−0.134

With Triplet on BChl 3

		contribution of BChl no.						
E_k cm^{-1} (nm)	μ^2 (D^2)	1	2	3	4	5	6	7
12270 (815.0)	134.1	**0.909**	−0.361	0	−0.175	0.004	−0.044	0.104
12289 (813.7)	67.5	0.161	−0.108	0	**0.875**	−0.243	−0.118	−0.353
12420 (805.1)	72.5	0.021	−0.108	0	0.298	0.298	**0.852**	0.290
12509 (799.4)	75.6	0.005	0.169	0	0.249	−0.313	−0.251	**0.865**
12618 (792.5)	26.6	0.383	**0.902**	0	0.041	0.130	0.086	−0.119
12718 (786.3)	37.1	−0.022	−0.066	0	0.229	**0.859**	−0.433	0.132

TABLE 5: Comparison of Excited State Energies (E_k) of This Study and the Literature

	E_k cm^{-1} (nm)		
BChl	this work	ref 5	ref 21
3	12121 (825.0)	12112 (825.6)	12111 (825.7)
1	12270 (815.0)	12266 (815.3)	12312 (812.2)
4	12310 (812.3)	12293 (813.5)	12278 (814.5)
6	12425 (804.8)	12396 (806.7)	12410 (805.8)
7	12509 (799.4)	12457 (802.8)	12488 (800.8)
2	12620 (792.4)	12496 (800.3)	12556 (796.4)
5	12718 (786.3)	12634 (791.5)	12610 (793.0)

TABLE 6: Comparison of Dipole Strengths $|\mu|^2$ of This Study and the Literature

BChl	this work $\lvert\mu\rvert^2$ (D^2)	ref 5 $\lvert\mu\rvert^2$ (D^2)	ref 21 $\lvert\mu\rvert^2$ (D^2)
3	45.9	46.7	49.7
1	147.4	151.5	60.6
4	58.0	57.2	138.8
6	92.1	89.3	100.3
7	70.5	90.7	71.1
2	30.2	11.7	26.7
5	38.1	35.5	34.6

for the $|D| + |E|$ transition (Figure 2C) the fit is in good agreement with the experiment.

The site energies of the 7 BChls are given in Table 3 along with the interaction energies that produced the best fits. We found that the parameter $\eta^2 = 1.9$. In Table 4, the eigenvalues, dipole strengths μ^2, and eigenvectors from the simulation are shown. The transition energies (cm^{-1}) and the dipole strengths found in this study, and the values from the literature, are listed in Tables 5 and 6, respectively.

Discussion

The present simulation procedure yields fits of the absorption and LD spectra of FMO that are about equally good as the fits presented in ref 5. The fit of the absorption spectrum of ref 5 in Figure 1D is better than in Figure 1A between 12 400 and 12 500 cm^{-1} and worse than in Figure 1A above 12 500 cm^{-1}. The fits of the LD spectrum of ref 5 in Figure 1E and ours in Figure 1B show a number of small differences, but overall the fits are equally good. Our fit of the CD spectrum (Figure 1C) is significantly better than that of ref 5 (Figure 1F). Notably, at the second highest peak in the experimental data (12500 cm^{-1}), the fit in Figure 1F is a minimum, while the fit in Figure 1C shows the experimentally observed positive peak.

Not unexpectedly, the fits of the T−S and LD(T−S) spectra obtained with the present simulation methods are dramatically improved compared with the fits of ref 5. In Figure 2A the fit to the T−S spectrum (calculated from the T−S(α) spectrum of ref 5) is much better than the fit of ref 5 to the T−S(α) spectrum (Figure 2D). (The T−S spectrum was, of course, not fitted in ref 5.) For example, the abrupt change from a positive peak at 12 270 cm^{-1} to a negative peak at 12 320 cm^{-1} peak is not well reproduced in Figure 2D, while this change is well fit in Figure 2A. In Figure 2E the LD(T−S) fit of ref 5 of the $|D| - |E|$ transition shows a negative peak where the spectrum shows a maximum (12 320 cm^{-1}). In Figure 2B this maximum is correctly reproduced. In the fit of the $|D| + |E|$ transition of the LD(T−S) spectum in Figure 2F the abrupt change from positive to negative at 12 290 and 12 310 cm^{-1} is not well reproduced, whereas in Figure 2C, better agreement is found.

In Table 3 the site energies and interaction energies are given. The values found for the interaction energies are approximately 25% higher than in ref 5 because we find a value of 1.9 for η, which is 20% lower than the value in ref 5. In refs 2, 3, and 5 the effective dipole strength of the noninteracting monomer was 28.7, 51.6, and 54.5, respectively. Our effective dipole strength is 36.3.

In Table 4 the eigenvalues, dipole strengths, and eigenvectors of the excitonic transitions that result from our simulation are presented. As in ref 5 we find that all eigenstates are dominated by a single BChl. The degree of delocalization on a pigment is given by the square of its coefficient in the eigenvector. In Tables 5 and 6, respectively, are the transition energies (cm^{-1}) and the dipole strengths found in this study, in comparison with literature values. The transition energies are similar in the three studies, except for the two bands at highest energy, which are 65−125 cm^{-1} (4.0−7.9 nm) higher in energy in the present study. The dipolar strengths found here agree with those of refs 5 and 21, except for the bands dominated by BChl 1 and 4, whose values are exchanged in ref 21 compared to ours and those of ref 5, and the bands dominated by BChl 7 and 2 which in ref 5 are approximately 27% higher and 41% lower, respectively, than our values and those of ref 21.

Conclusions

The absorption, LD, CD, and the ADMR-detected T−S and LD(T−S) spectra of *P. aestuarii* have been simultaneously fit with an exciton model. A previous analysis in ref 5 included angle-dependent T−S(α) spectra which were interpreted as isotropic T−S spectra. Taking the correct angle-dependence into account, we find significantly improved fits and about 25% higher interaction energies than found in ref 5. We conclude that simultaneous fitting of all available optical (difference) spectra with correct procedures offers a precise, detailed description of pigment−pigment interactions in a pigment−protein complex.

Acknowledgment. The authors thank F. van Mourik, H. Vasmel, and R. J. W. Louwe for supplying their experimental data. This work has been supported by Chemische Wetenschappen (CW), financed by The Netherlands Organization for Scientific Research (NWO).

References and Notes

(1) Tronrud, D. E.; Schmidt, M. F.; Matthews, B. W. *J. Mol. Biol.* **1986**, *261*, 443.
(2) Pearlstein, R. M. *Photosynth. Res.* **1992**, *31*, 213.
(3) Lu, X.; Pearlstein, R. M. *Photochem. Photobiol.* **1993**, *57*, 86.
(4) Gülen, D. *J. Phys. Chem.* **1996**, *100*, 17683.
(5) Louwe, R. J. W.; Vrieze, J.; Aartsma, T. J.; Hoff, A. J. *J. Phys. Chem. B* **1997**, *101*, 11280.
(6) Owen, G. M.; Hoff, A. J. *J. Phys. Chem. B* **2000**, *104*, 2775.
(7) Louwe, R. J. W.; Vrieze, J.; Aartsma, T. J.; Hoff, A. J. *J. Phys. Chem. B* **1997**, *101*, 11273.
(8) Van Mourik, F.; Verwijst, R. R.; Mulder, J. M.; Van Grondelle, R. *J. Phys. Chem.* **1994**, *98*, 10307.
(9) Vasmel, H.; Swarthoff, T.; Kramer, H. J. M.; Amesz, J. *Biochim. Biophys. Acta* **1983**, *725*, 361.
(10) Den Blanken, H. J.; Jongenelis, A. P. J. M.; Hoff, A. J. *Biochim. Biophys. Acta* **1983**, *725*, 472.
(11) Den Blanken, H. J.; Hoff, A. J. *Chem. Phys. Lett.* **1983**, *98*, 255.
(12) Pearlstein, R. M. In *Chlorophylls*; Scheer, H., Ed.; CRC Press: Boca Raton, 1991; p 1047.
(13) Knapp, E. W.; Scherer, P. O. J.; Fischer, S. F. *Biochim. Biophys. Acta* **1986**, *852*, 295.
(14) Tinoco, I. In *Advances in Chemical Physics*; Prigogine, I., Ed.; Interscience Publishers: New York, 1962; Vol. IV, p 113.
(15) Struve, W. S. In *Anoxygenic Photosynthetic Bacteria*; Blankenship, R. E., Madigan, M. T., Bauer, C. E., Eds.; Kluwer Academic Publishers: Dordrecht, 1995; p 297.
(16) Gouterman, M. *J. Mol. Spec.* **1961**, *6*, 138.
(17) Olson, J. M. In *The Chlorophylls*; Academic Press: New York, 1966; p 161.
(18) We follow a recent treatment by Prof. R. S. Knox (to be published), where it is shown that by using the experimentally determined dipole strength the local field correction is taken care of: the dipole−dipole interaction is then proportional to η^2.
(19) Johnson, S. G.; Small, G. J. *J. Phys. Chem.* **1991**, *95*, 471.
(20) Vulto, S. I. E.; Strelsov, A.; Aartsma, T. J. *J. Phys. Chem. B* **1997**, *101*, 4845.
(21) Vulto, S. I. E.; De Baat, M. A.; Neerken, S.; Nowak, F. R.; Van Amerongen, H.; Amesz, J.; Aartsma, T. J. *J. Phys. Chem. B* **1998**, *102*, 10630.